Composite metasurface for surface wave radar enhancement

Briand Gildas, André Barka, Shah Nawaz Burokur

Composite metasurface for surface wave radar enhancement

Gildas Briand
DEMR, ONERA, Université de Toulouse
Toulouse, France
gildas.briand@onera.fr

André Barka
DEMR, ONERA, Université de Toulouse
Toulouse, France
andre.barka@onera.fr

Shah Nawaz Burokur
LEME, Univ. Paris Nanterre
Ville d'Avray, France
sburokur@parisnanterre.fr

***Abstract*—This paper presents the design, fabrication and experimental validation of a compact composite metasurface for a surface wave radar. The ultimate aim is to enhance the surface wave excitation efficiency of a HF-band surface wave radar by modifying the radiation characteristics of the emitting antenna using a highly inductive metasurface. A reduced-scale prototype is presented here in L-band to prove the validity of this concept.**

***Index Terms*—HFSWR, radar, antenna, metasurface, composite**

I. Introduction

High-frequency surface wave radars represent an effective solution for maritime surveillance. Indeed, with a theoretical range of approximately 400 km, they can cover the entire Exclusive Economic Zone (EEZ), an area where France holds rights to oil, mineral, and fishing exploitations. Due to the strategic importance of these zones, as well as to prevent illegal activities and ensure faster assistance to distressed vessels, high-frequency (3 – 30 MHz) surface wave radars are destined to be deployed both in mainland and overseas territories. Surface wave radars have been employed by major military powers since the Cold War in France, tests have been carried out in the 2000s [1]. During these trials, interference resulting from wave reflection off the ionosphere was deemed problematic [2]. Consequently, a metamaterial was proposed to reduce propagation towards the sky and enhance surface wave power [3], [4]. Despite satisfactory results, this structure remains too tall (3 m – λ/10 at 10 MHz) compared to current coastal regulations in France. Finally, a more compact metasurface with a thickness of 10.26 mm, corresponding to λ/27, was proposed at 1.1 GHz [5]. It fulfils the same objectives and exhibits performance comparable to the previous solution at 10 MHz. However, its realization depends on a high-permittivity, low-loss substrate, yet to be identified in the HF band.

In this communication, we present the design of a composite and compact metasurface at 1.1 GHz. Particular attention has been paid to developing a composite material which is feasible in the HF band. With a structure height of λ/27 (10.26 mm at 1.1 GHz) and composed of materials making the structure feasible to develop in HF, the proposed metasurface would achieve a vertical electric field gain of 8 dB at 100 m, as defined by the gain specific to this application (see Eq. 6). This contribution is structured as follows. Section 2 presents the design of the composite metasurface along with the 1/100 scale prototype. Section 3 outlines the simulated performances in the near-field of the metasurface. Finally, Section 4 concludes on the results obtained, highlighting the role of the metasurface.

II. Composite metasurface

A. Composite dielectric design

The specifically designed composite dielectric material is shown in Figure 1. It is made of three successive layers of PTFE (Polytetrafluoroethylene, commonly known as Teflon), distilled water supposed to have low losses, and PTFE along the y-axis. The composite is shown in Figure 1 where p the spatial period of the unit cell, l_w is the length of water, l_p the length of PTFE, f is the volume fraction of the composite defined by $f = \frac{l_w}{l_w+2l_p}$ and h is the thickness (height) of the substrate. Initially, we aim to determine the necessary proportion of distilled water within the PTFE to achieve a permittivity of $\varepsilon_{\text{eff}} = 6$, considering $\varepsilon_{\text{ptfe}} \approx 2.1$ and $\varepsilon_{\text{water}} \approx 78.4$. In [5], it has been shown that a substrate permittivity of 6 was mandatory for this substrate thickness in order to get the highly inductive metasurface behaviour. It is estimated that a volume fraction f of 0.05 would be required to obtain the desired effective permittivity, representing a distribution of 5% distilled water and 95% PTFE, according to the following mixing law [6] :

$$\varepsilon_{\text{effx}} = \varepsilon_{\text{effz}} = f\varepsilon_{\text{water}} + (1-f)\varepsilon_{\text{ptfe}} \tag{1}$$

$$\varepsilon_{\text{effy}} = \frac{\varepsilon_{\text{water}}\varepsilon_{\text{ptfe}}}{(1-f)\varepsilon_{\text{water}} + f\varepsilon_{\text{ptfe}}} \tag{2}$$

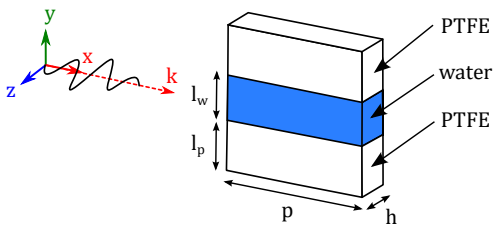

Fig. 1: Composite-based dielectric material made with water and PTFE

B. Unit-cell design

For the metasurface, we employ the elementary pattern used previously [5], represented in Figure 3a. We consider its operation in a highly inductive regime as depicted in the model illustrated in Figure 2a and proposed in [7]: L_a and C_a represent the equivalent inductance and capacitance of the square ring, respectively, and are given by

$$L_a = \frac{\mu_0 d}{2\pi} \log\left(\csc\left(\frac{\pi e}{2p}\right)\right) \tag{3}$$

$$C_a = \frac{2\varepsilon_0 \varepsilon_e d}{\pi} \log\left(\csc\left(\frac{\pi g}{2p}\right)\right) \tag{4}$$

with the unit cell period $p = 34$ mm, the unit cell height h, the loop width d, the inner loop width d_i, $e = \frac{(d-di)}{2}$, $g = (p-d)$, $\varepsilon_e = \frac{\varepsilon_r+1}{2}$, ε_0 the free space permittivity, μ_0 the free space permeability, csc the cosecant trigonometric function and Z_d the equivalent impedance of the dielectric given by equation 2.45c in [8].

$$Z_d = jZ_0\sqrt{\frac{\mu_r}{\varepsilon_r}}\tan\left(\omega c\sqrt{\mu_r\varepsilon_r}h\right) \tag{5}$$

where Z_0 is the free space characteristic impedance.

The parameter to be varied here is the thickness of the dielectric used for the metasurface. Using the analytical model and electromagnetic simulations (such as Floquet simulation in CST MWS), a substrate thickness of 10.26 mm is set as in [5]. Figure 2b presents the reactance obtained for this dielectric height.

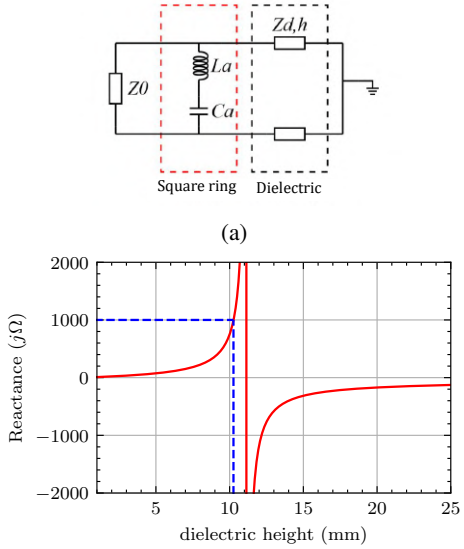

Fig. 2: (a) Equivalent transmission line circuit model of the square loop. (b) Reactance versus composite dielectric height of the unit cell at 1.1 GHz. The blue dashed line represents the reactance for h = 10.26 mm

The proposed unit cell of the metasurface is shown in Figure 3a. The optimised dimensions are $h = 10.26$ mm, $d = 31.7$ mm and $d_i = 8.04$ mm. For fabrication purposes, a PTFE bottom and cap are used to contain the water within the trench in the PTFE volume.

To achieve performance comparable to previous works, a metasurface consisting of 5 × 12 unit cells is considered. The metasurface is composed of two parts: a F4BM220 dielectric substrate with a permittivity of $\varepsilon_r = 2.2$ and a loss tangent of $\tan\delta = 0.0022$, on which the copper patterns are printed; and a PTFE (Teflon) plate with a permittivity of $\varepsilon_r = 2.1$ and a loss tangent of $\tan\delta = 0.0002$. A PTFE mechanical frame and a silicone seal have been added to retain water in the machined trenches. Similarly, nylon screws are used to bolt the substrate onto the PTFE plate, as illustrated in Figure 3b.

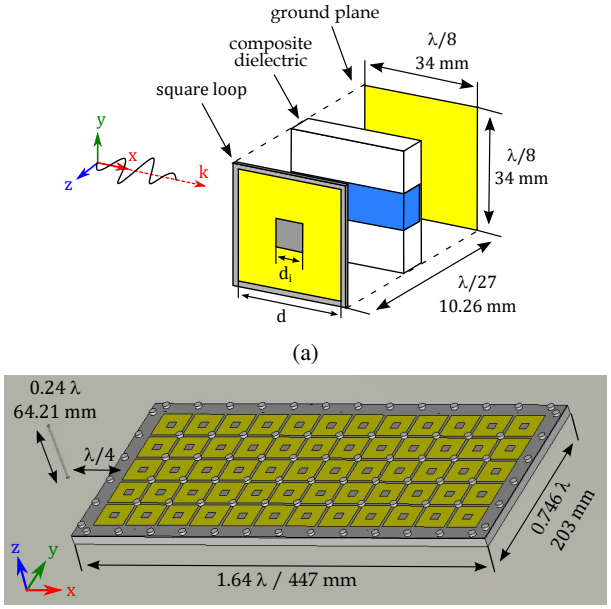

Fig. 3: (a) Proposed metasurface unit-cell. (b) Composite proposed metasurface and its monopole emitting antenna.

III. Performance and Measurements of the Metasurface

A. Expected metasurface gain

The objective of the metasurface is to increase the vertical component E_z of the electric field in front of the metasurface and at the ground level. We use a quarter-wavelength monopole antenna to excite a vertical electric field. Its simulated impedance matching as a function of frequency is presented in Figure 4a. The performance of the metasurface is evaluated by comparing the electric field surrounding the antenna with and without the metasurface. Electromagnetic simulations are conducted using both frequency and time-domain solvers in the CST Microwave Studio software. The monopole is fed by a discrete port with a 50 Ω impedance.

Open boundary conditions are applied around the simulated structure.

Following the initial simulations, a significant frequency shift associated with the estimation of the required volume of water to achieve an effective permittivity $\varepsilon_r = 6$ is observed. This is primarily due to the non-adapted equivalent model of the square ring for use with a composite dielectric material and secondarily due to the use of a low number of periods within the metasurface. Therefore, the volume fraction of water was readjusted through parametric simulations to achieve the most optimal operating regime. The optimized configuration consists of 25% distilled water and 75% PTFE.

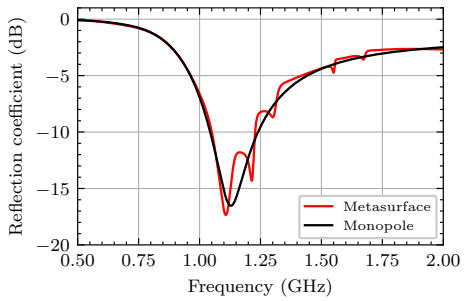

(a)

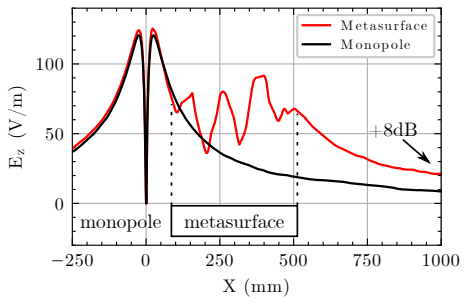

(b)

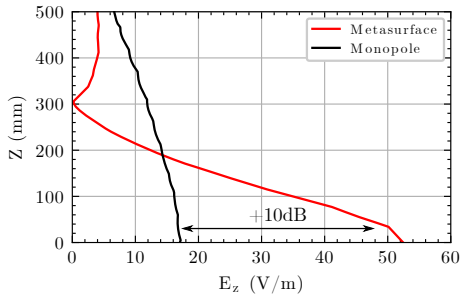

(c)

Fig. 4: Simulation results. (a) Impedance matching of the monopole alone and in presence of the composite metasurface. (b) Electric field E_z along X-axis from the monopole and at the end of the metasurface (Y = 0 mm, Z = 30 mm). (c) Electric field E_z along Z-axis from the ground plane. It shows the electric field in the ground (X = 590 mm, Y = 0 mm)

In this case, the simulated impedance matching of the monopole antenna in the presence of the metasurface is nearly identical to that of the monopole alone, except for some coupling effects between the metasurface and the monopole (Figure 4a). Figure 4b presents the electric field level with and without the metasurface along the X-axis with Z = 30 mm and Y = 0 mm. Similarly, Figure 4c presents the electric field level with and without the metasurface along the Z-axis at X = 590 mm and Y = 0 mm. By comparing the simulation results with the previous prototype [5], comparable field levels are observed. The gain is defined as:

$$Gain_{\text{MS}} = 20\log_{10}\left(\frac{E_{\text{MS}}}{E_{\text{monopole}}}\right) \tag{6}$$

with E_{MS} being the vertical electric field of the monopole with the metasurface, and E_{monopole} representing the field of the monopole without the metasurface. It can be observed that the metasurface provides a gain of 8 dB at 1 m from the monopole, at a height of 30 mm and 10 dB above the ground at a distance of 590 mm from the monopole. This significant increase in the electric field enhances the efficiency and directivity of the antenna system.

B. Experimental testing of the metasurface

In order to experimentally validate the concept, a prototype has been fabricated. The square loops are made through chemical etching on an F4BM220 substrate (the same as in simulation). A photograph of the sample is presented in Figure 5a. A block of PTFE (Teflon) is machined, and trenches with a width of 10 mm are made to retain distilled water, as shown in Figure 5b. Holes are also drilled to secure the metasurface onto the PTFE block. Additionally, a silicone sponge seal with a diameter of 2 mm between the substrate shown in Figure 5a and the machined PTFE plate in Figure 5b improves the metasurface sealing. To evaluate the performance of the fabricated prototype, a test setup has been assembled. The metasurface will be placed on a ground plane (1 m × 2 m, equivalent to $3\lambda \times 5\lambda$) in front of a monopole tuned to 1.1 GHz.

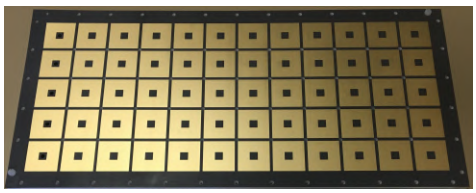

(a)

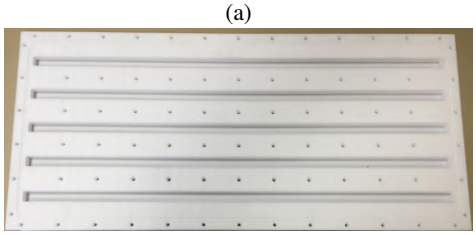

(b)

Fig. 5: (a) Top cover F4BM220 substrate (b) Bottom plate machined PTFE

The reflection coefficient (S_{11}) of the metasurface has been measured using a HP 8753ES network analyzer as shown in Figure 6. Moreover, when comparing Figure 4a and Figure 6, it can be clearly observed that the measured composite metasurface has no influence on the reflection coefficient of the monopole antenna.

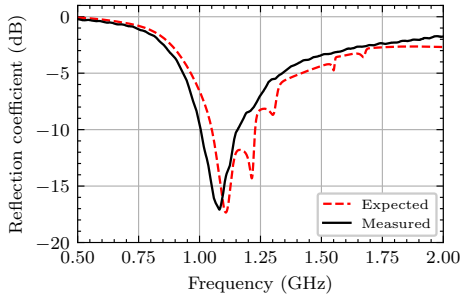

Fig. 6: Measured and simulated impedance matching of the monopole with the metasurface.

Figure 7a shows how the electric field in front of the metasurface is measured. Electromagnetic infrared thermography imaging [9], [10] has been used to validate the metasurface behaviour (see Figure 7b). The setup measurement used a TELEOPS-IR 2K infrared camera and a 50 W 1.1 GHz power amplifier has been used to feed the monopole antenna.

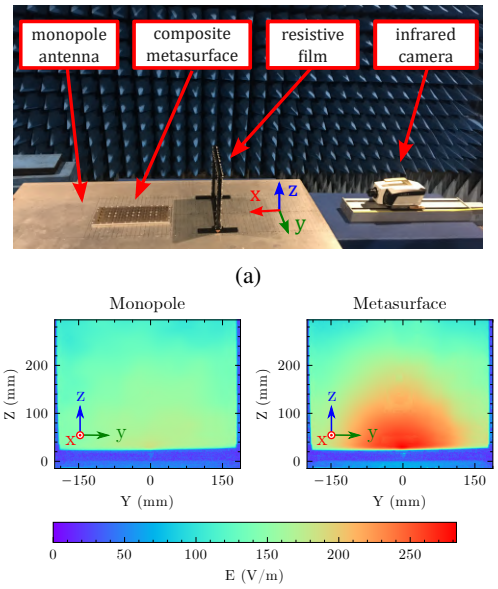

(a)

(b)

Fig. 7: (a) Electric field measurement setup using infrared thermography imaging (b) Electric field screens of the monopole with and without the metasurface. Measured using infrared thermography at X = 550 mm.

Intermediate measurement results have shown significantly lower performance than simulation results, as shown in Figures 8a and 8b. Scanning area is limited in Figure 8a due to a non-adapted resistive film support to measure E_z over the metasurface.

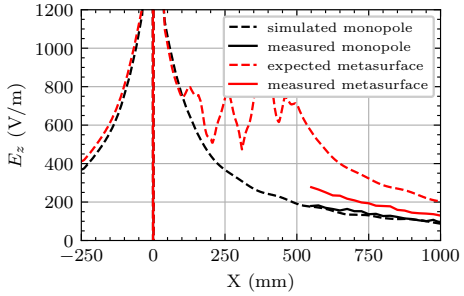

(a)

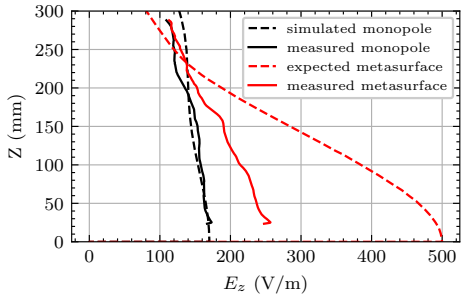

(b)

Fig. 8: Measurement and simulation results. (a) Electric field E_z along X-axis. (b) Electric field E_z along Z-axis from the ground plane.

There are some uncertainties about the quality of the water used during the experiment and the losses incurred. Table I shows the conductivity of different types of water. Using the Klein & Swift [11] analytical model of water with salinity content, we can find an estimated loss factor (tan δ) for each type of water.

Type of water	Conductivity (μS/cm)	Est. Loss factor (tan δ)	Source
Distilled	0.5 - 5	7.16×10^{-2}	[12]
Demineralized	5 - 30	7.19×10^{-2}	[13]
Drinking	30 - 800	8×10^{-2}	[13]
Slightly saline	700 - 2000	9.9×10^{-2}	[14]
Moderately saline	2000 - 10000	19.4×10^{-2}	[14]
Highly saline	10000 - 25000	42.9×10^{-2}	[14]

TABLE I: Different type of water with associated conductivity and estimated loss factor

The Klein & Swift analytical model takes as input the total dissolved solids (TDS in part per million, ppm) for water salinity and the liquid temperature. The average electrical conductivity (μS/cm) is converted to total dissolved solids using a k_e factor ranging from 0.5 to 0.65 [15]. The room temperature during the electric field measurement performed on the prototype was 14.3°C.

A parametric full-wave simulation has been done using CST MWS by varying the loss factor (tan δ) for different type of water. The results are displayed as reflection coefficient of

the monopole in presence of the metasurface (Figure 9) and as the gain of the metasurface (Eq. 6) along X and Z axis (respectively Figure 10a and Figure 10b).

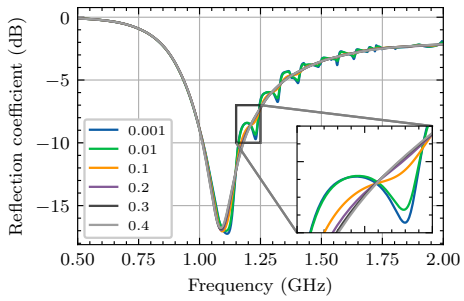

Fig. 9: Impedance matching of the monopole with the metasuface by varying the loss factor of the water.

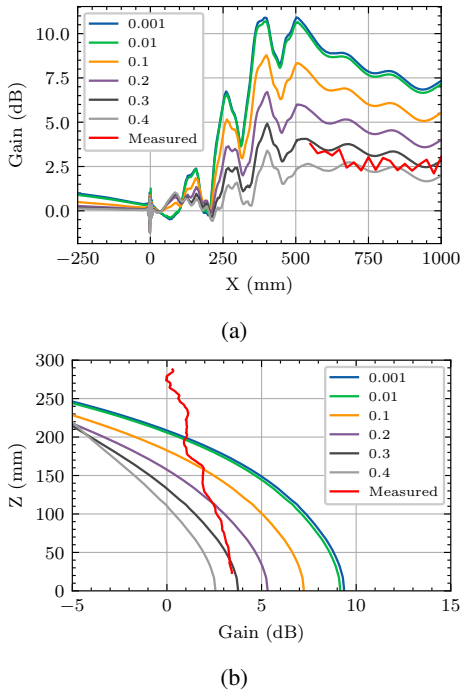

Fig. 10: Measurement and simulation results for different loss factor of the water. (a) Gain of the metasurface along X-axis. (b) Gain of the metasurface along Z-axis from the ground plane.

Retro simulation results show that the concept is very sensitive to the losses of the water used. Figure 9 shows that the greater the losses in the water, the more the coupling effects between the metasurface and the monopole are attenuated. Figures 10a and 10b tend to show equivalent loss factor in the order of $\tan\delta \approx 0.3$. However, it seems unlikely that the water used for the measurements has a saline concentration close to a moderately saline water. Waveguide measurements of the water used and commercially purchased distilled water samples are in progress. It is likely possible that the losses in the metasurface are also due to other factors.

IV. Conclusion

This study has presented the design of a metasurface with a composite substrate to modify the radiated field of a monopole antenna for surface wave radar applications. The proposed setup presents a simulated gain of 10 dB at the ground level and in front of the metasurface. The proposed metasurface is compact compared to other metasurfaces proposed for this application while being realizable in the HF band due to the materials used for the composite dielectric material. The results of the upcoming measurements will be presented during the conference. Note that this composite concept remains very sensitive to the substrate losses. This point is crucial for future realization in the HF band which is why we are also conducting research into fully metallic and dielectric substrate-free solutions.

Acknowledgment

This work is cofunded by the Innovation Defence Agency (AID) from the French Ministry of Defence and ONERA, the French Aerospace Lab.

References

[1] M. Menelle, G. Auffray, and F. Jangal, "Full digital high frequency surface wave radar: French trials in the Biscay bay," in *2008 International Conference on Radar*. Adelaide, SA: IEEE, Sep. 2008.

[2] M. J. Abi Akl, F. Jangal, M. Darces, and M. Helier, "Modelling the ionospheric effects in HF radar long term integration," in *2016 10th European Conference on Antennas and Propagation (EuCAP)*. Davos, Switzerland: IEEE, Apr. 2016, pp. 1–4.

[3] Q. Herbette, N. Bourey, M. Menelle, M. Darces, S. Saillant, and M. Helier, "Using a 3D metamaterial to enhance surface wave propagation in HF band," in *2021 15th European Conference on Antennas and Propagation (EuCAP)*. Dusseldorf, Germany: IEEE, Mar. 2021.

[4] Q. Herbette, N. Bourey, M. Menelle, M. Darces, S. Saillant, Y. Chatelon, and M. Hélier, "Antenne HF à métamatériau : un défi technologique relevé pour améliorer les performances d'un radar de surveillance maritime à ondes de surface," in *XXII èmes Journées Nationales Microondes*, Limoges, Jun. 2022, pp. 157–161.

[5] A. Barka and D. Prost, "Low-profile inductive metasurface for surface wave excitation in L-band: design, manufacture and electromagnetic infrared measurements," *Advanced Electromagnetics*, vol. 11, no. 2, pp. 49–53, Jun. 2022.

[6] V. A. Markel, "Introduction to the Maxwell Garnett approximation: tutorial," *Journal of the Optical Society of America A*, vol. 33, no. 7, p. 1244, Jul. 2016.

[7] D. Ferreira, R. F. S. Caldeirinha, I. Cuinas, and T. R. Fernandes, "Square loop and slot frequency selective surfaces study for equivalent circuit model optimization," *IEEE Transactions on Antennas and Propagation*, vol. 63, no. 9, pp. 3947–3955, Sep. 2015.

[8] D. M. Pozar, *Microwave engineering*, 4th ed. Wiley, 2012.

[9] D. Prost, "Measurement of the amplitude and polarization of the electric field by electromagnetic infrared thermography," *IEEE Transactions on Antennas and propagation*, vol. 70, no. 5, 2022.

[10] T. Crépin, F. Issac, D. Prost, and S. Bolioli, "Microwave electric field imaging of metamaterials using thermoemissive films," *IEEE Antennas and Propagation Magazine*, vol. 56, no. 3, Jun. 2014.

[11] L. Klein and C. Swift, "An improved model for the dielectric constant of sea water at microwave frequencies," *IEEE J. Ocean. Eng.*, vol. 2, no. 1, pp. 104–111, Jan. 1977.

[12] "Specification for reagent water," ASTM D1193-06, ASTM International, Standard, 2018.

[13] Eurowater. [Online]. Available: https://www.eurowater.com/en/water-quality

[14] J. D. Rhoades, A. Kandiah, and A. M. Mashali, *The use of saline waters for crop production*. New York, NY: Artabras, 1992.

[15] Eutech Instruments. Conductivity to TDS conversion factors. in tech tips. [Online]. Available: https://www.eutechinst.com/tips/contds/07.pdf